Mon. Not. R. Astron. Soc. **000**, 000–000 (0000) Printed 5 February 2008 (MN LATEX style file v1.4)

Comments on the superluminal motion in Cygnus X-3

R. N. Ogley⋆[1], S. J. Bell Burnell[1] and S. J. Newell[2]
[1] *Department of Physics, The Open University, Milton Keynes, UK.*
[2] *NRAL, Jodrell Bank, Macclesfield, Cheshire, UK.*

5 February 2008

ABSTRACT
Following the recent discovery that Cyg X-3 exhibits superluminal motion, the implications of superluminal expansion and contraction are investigated. We propose that the effect is due to either a propagating photon pattern or to outwardly moving shells illuminated by an intense beam of radiation.

Key words: stars: individual : Cyg X-3 – binaries: close

1 INTRODUCTION

Since its discovery in 1966 (Giacconi et al. 1966) Cyg X-3 has remained one of the most unusual and enigmatic objects in the sky. A neutron star–Wolf Rayet binary system, Cyg X-3 exhibits the following unusual properties: major radio flares at intervals of aproximately 18 months (Waltman et al. 1995); a 4.8 hour period making it the shortest period high mass X-ray binary; and following a major flare, radio jets which expand at $0.35c$ (Spencer et al. 1986).

Recently Newell, Garrett & Spencer (1996, hereafter NGS; Newell 1996) published VLBA maps showing superluminal motion at a significantly higher magnitude than previous superluminal velocities in the galaxy. The system also displayed superluminal contraction. We consider models for this behaviour.

2 SUPERLUMINAL MOTION

Superluminal expansion in one-sided quasars has been well documented and we use the same notation here. Consider a blob of material emitted at a velocity v at an angle θ to the line of sight; the blob appears to travel normal to the line of sight with a velocity $v_{\rm app}$ given by

$$v_{\rm app} = \frac{v \sin\theta}{1 - \beta\cos\theta} \qquad (1)$$

where $\beta = v/c$. For a given β the angle at which the maximum superluminal effect occurs is given by $\cos\theta_{\rm max} = \beta$ and at this angle the apparent velocity has a maximum of $\beta_{\rm app}({\rm max}) = \gamma\beta$ where we have substituted $\gamma = (1-\beta^2)^{-1/2}$.

Flare	Motion	Axis	$\beta_{\rm app}$	β	γ
1	Expansion	Major	2.45 ± 0.55	0.920	2.56
		Minor	0.84 ± 0.09	0.579	1.23
	Contraction	Major	2.97 ± 0.33	0.947	3.12
		Minor	2.53 ± 0.32	0.926	2.65
2	Expansion	Major	4.75 ± 0.42	0.979	4.88
		Minor	2.32 ± 0.32	0.914	2.46
	Contraction	Major	6.76 ± 0.72	0.989	6.86
		Minor	2.53 ± 0.54	0.926	2.65

Table 1. Apparent and actual velocities along the axes of the ellipse

3 CYGNUS X-3 RESULTS

Observations by NGS of Cygnus X-3 showed that it was undergoing apparent superluminal expansion and contraction on both the major and minor axes of an ellipse. The observations include frames showing the object at intermediate size. Taking $\beta_{\rm app}({\rm max}) = \beta_{\rm app}$ and using the $\beta_{\rm app}$ values quoted by NGS, we find β and γ as reported in Table 1. Using $\beta_{\rm app}({\rm max})$ for $\beta_{\rm app}$ will tend to underestimate the actual velocities. The $\beta_{\rm app}$ values reported by NGS may also be underestimates of the superluminal velocities (see section 4.2). We assume that the distance adopted by NGS for Cyg X-3 is not seriously in error.

Questions that arise are:

- What is moving? Is it material moving out and radiating, or is it a pattern of radiation illuminating fixed material?
- Do any realistic models produce contraction?
- Why are the speeds of expansion and contraction different, with contraction being the faster? Why does the second flare give greater speeds?
- Why is the shape elliptical and not circular?

⋆ E-mail: R.N.Ogley@open.ac.uk

4 CYGNUS X-3 MODELS

We describe a variety of models which attempt to explain the superluminal expansions and contractions shown in Table 1 along with the observed elliptical shape. A jet of radio-emitting plasma, an expanding radiating shell, a beam of highly energetic particles or radiation striking a stationary medium and exciting it, and a pattern of radiation are considered. We do not attempt to explain how such conditions arise, nor do we consider radiation or cooling mechanisms.

4.1 Bipolar jet model

Superluminal expansion has been observed in the galactic bipolar jet sources GRS 1915+105 (Mirabel & Rodríguez 1994) and GRO 1655-40 (Tingay et al. 1995). Although the expansion velocities observed here are much larger, could such a model explain the superluminal expansion of Cyg X-3? To explain superluminal *contraction* however by a similar process the bulk motion of the material would have to be reversed, which is unrealistic. Nor does this model account readily for the elliptical shape of the emission. It is worth noting that while this model does not account for the motion in Cygnus X-3, it is consistent with the relativistic motions in GRS 1915+105 and GRO J1655-40 and cannot be discounted for these sources.

Before moving to the next model, note that an apparently superluminal blue-shifted jet is accompanied by an apparently subluminal red-shifted jet. In obtaining their values for $\beta_{\rm app}$ NGS assumed that the apparent expansion (or contraction) was from (or to) a central point, and of equal magnitude in opposite directions. Thus the superluminal speeds have probably been underestimated. This is developed further in the next section.

4.2 Offset centre

A consequence of the hybrid mapping technique used by NGS is that absolute positional information is lost and so it is not possible accurately to locate the ellipses relative to each other or to the core of the system. NGS assume that the bright core of each map represents the same feature.

If the superluminal expansion speeds along the major axis are caused by a bulk motion with a component towards the observer, then the speed in the opposite direction must be subluminal, and the point from which the expansion takes place must be offset from the observed centre of the major axis. The same argument applies to motion along the minor axis. The source of the expanding material is located at or near the rim of the ellipse, lying on neither its major nor minor axis, and the superluminal expansion speeds are thus approximately doubled (Table 2)

An outburst might produce an elliptical lobe with the central source lying at one end of the major axis of the ellipse, but seems unlikely to do so for the central source offset from both the major and minor axes. In addition this model does not readily explain the superluminal contraction. We set this model aside.

Axis	$\beta_{\rm app}$	$\beta'_{\rm app}$	β'	γ'
Major	4.8	9.6	0.995	9.64
Minor	2.3	4.6	0.977	4.68

Table 2. Projected velocities and true velocities based on a shifted expansion centre based on flare 2.

4.3 Christmas tree model or propagating photon pattern

The velocities found in the previous models are at the limit of physical reality. If, however, the superluminal effect is caused by a pattern of photons propagating, then relativistic bulk motion, and the reversal of relativistic bulk motion may not be necessary. Equation 1, with $v = c$ applies.

If an intense burst of radiation was emitted from the core of Cyg X-3 the observer might, in addition to seeing some of these photons directly, see either photons reflected/scattered off surrounding material or secondary photons generated in this material following excitation by the burst of radiation. The size of the emitting patch would be governed by the extent of the distribution of material around the core of Cyg X-3, by the distance from the core that the burst of radiation had travelled and possibly by the excitation time for the case of secondary photons.

It is possible to envisage an expanding patch of emission, growing as the burst of radiation travels further out. The maximum size observed is determined by the duration of the burst or by the extent of the surrounding material or (less likely) by the optical depth of the surrounding material to the centrally emitted radiation. Note however that equation 1 is cylindrically symmetric about the line of sight, so that an isotropic burst of radiation into an isotropic distribution of surrounding material would give a circular patch of emission. The observed elliptical shape could be produced if either the burst of radiation or the surrounding material were confined to a disc inclined to the line of sight. Equation 1 requires that the total apparent expansion speed along any axis is $\geq 2c$, and the observations satisfy this. Along the axis of the ellipse that lies in the plane of the sky the total apparent expansion speed takes the minimum value of $2c$. With higher signal-to-noise observations it should be possible to identify this axis and determine the orientation of the disc in space.

The superluminal contraction, in this model, is most likely explained by a steady reduction in the effective extent of the photon pattern. Either the central intensity drops continuously and insufficient radiation reaches the outer areas to make visible the material there, or (less likely) a steady change of the central wavelength makes the optical depth gradually greater. It is unlikely that the extent of the surrounding material shrinks superluminally. Another possibility is that we are seeing the cooling of an excited region after the central radiation has turned off. However if the radiation ceases totally, the central parts of the patch cool first. This is not what is observed.

4.4 Searchlight beam model

If a conical jet of high energy photons or particles was ejected from the Cyg X-3 core, and there was some absorption by

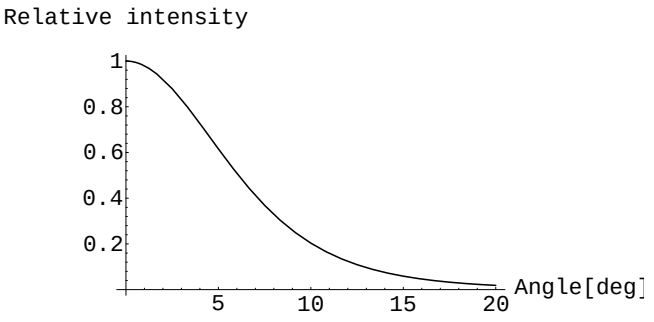

Figure 1. Plot of Doppler boosted intensity against offset angle. For a dynamical range of 32, the maximum angle at which flux is detected is 17.6 degrees. The plot is for the major axis of the second flare; $\gamma = 4.88$.

material in a surrounding stationary spherical shell, then that part of the shell intersected would become excited and radiate. If the conical beam is inclined to the line of sight then the observed emission patch has an elliptical shape. For flare 2 the required eccentricity is produced if the cone axis is at an angle of 61° to the line of sight. If the inclination varies by $\sim 10°$ then the observed changes in eccentricity can be accommodated. The observed emission is centrally peaked suggesting that the beam also is more intense along its central axis.

The apparent superluminal expansions and contractions could be produced by relatively small expansions and contractions of the opening angle of the cone, provided that the heating and cooling time constants are less than the timescales for the change of cone angle. The confinement of the beam might be by a magnetic throat, with the opening angle in part governed by the flux in the beam, producing the observed correlation beween size and intensity of the emission.

Alternatively, at least a part of the expansion and contraction could be produced by the weaker emission from the edge of the ellipse rising above and falling below a detection threshold.

4.5 Doppler boosted spot on an expanding shell

Consider a spherical shell of material expanding relativistically at fixed velocity V. The emission from material travelling at small angles, ϕ, to the line of sight will have its intensity Doppler boosted according to

$$I(\phi) = \frac{I'(\phi)}{\gamma^3 \left(1 - \beta \cos\phi\right)^3} \qquad (2)$$

where $I'(\phi)$ is the intensity in the rest frame of the radiating material (Rybicki & Lightman, 1979). Assuming $I'(\phi)$ to be constant, a plot of observed intensity with angle is shown in Figure 1. The shell appears to have a bright spot centred on our line of sight, which expands as the shell expands.

Let r be the radius of the shell at time t, and α the angular diameter of the spot (Figure 2). The shell is expanding at a velocity $V = \delta r/\delta t$ and the observed expansion of the spot can be written as $v = \delta\alpha/\delta t$. Therefore $\sin\phi = \alpha/r = \delta\alpha/\delta r$, hence $V = (r/\alpha)\, v$ giving $v < V$. To find (r/α), we use the dynamical range of the *VLBA* images to give the limit at which lack of Doppler boosting is unable to bring the intensity up to detectable levels.

Axis	$\beta_{\rm app}$(spot)	$\beta_{\rm app}$(shell)	β(shell)	γ(shell)
Major	4.8	15.8	0.998	15.8
Minor	2.3	7.58	0.991	7.63

Table 3. Adjusted velocities for a shell of material with a Doppler boosted spot

The dynamical range for the VLBA images in Cyg X-3 is 32:1 which would imply from Figure 1 that any flux outside the angle of 17.6° is undetectable. The profile used for this assumes $\gamma = 4.88$. If $\phi = 17.6°$ then $(r/\alpha) = 3.30$ which implies shell speeds for the second flare as shown in Table 3.

In this model a spherical shell will produce a circular spot with circular expansion velocities. To simulate the elliptical shape observed we postulate a shell distorted by expansion into an anisotropic dense medium.

A dense medium, sufficient to decelerate the shell, is required to explain the contraction. In this model the apparent contraction is due to a rapid reduction in intensity, lowering the emission from most of the spot area below the detection threshold. The rapid reduction in intensity is due to the collapse of the Doppler boosting when the expansion velocity drops.

A reduction in Doppler boosting of the intensity of 1/32 would require a velocity change of $\delta\beta = -0.819$. If this occurs in $\sim$ 60 minutes (the typical time between contractions in the NGS observations) then the retardation is ~ 70 km s^{-2} and the shell pushes back the retarding medium by $\sim 900 R_\odot$. Considerable energy would be transfered to the medium, presumably with detectable consequences.

4.6 Illuminated shells

This hybrid model, which combines the useful features of the moving shell and the searchlight beam models (§§ 4.4 and 4.5) best addresses the difficult questions concerning the contraction and the elliptical shape of the emitting area.

The central source produces a series of expanding spherical shells, and a beam of energetic particles or photons. The beam, which is inclined to the line of sight, illuminates a patch on an expanding shell which is seen as an elliptical area of emission. As the shell expands the area expands superluminally, as set out in § 4.5, with the minor axis expansion velocities apparently smaller than the major axis ones. Doppler boosting of the intensity is not significant here because of the large angle to the line of sight.

However, as the shell expands the illuminating beam intensity per unit area decreases and so the emitted radiation falls. If the intensity of the emission across the area has a flat distribution and is close to the detection threshold of the observer's equipment then as the source fades its detectable area will rapidly shrink simulating superluminal contraction.

Meanwhile another shell has been produced and is expanding in the wake of the first. As emission from the first

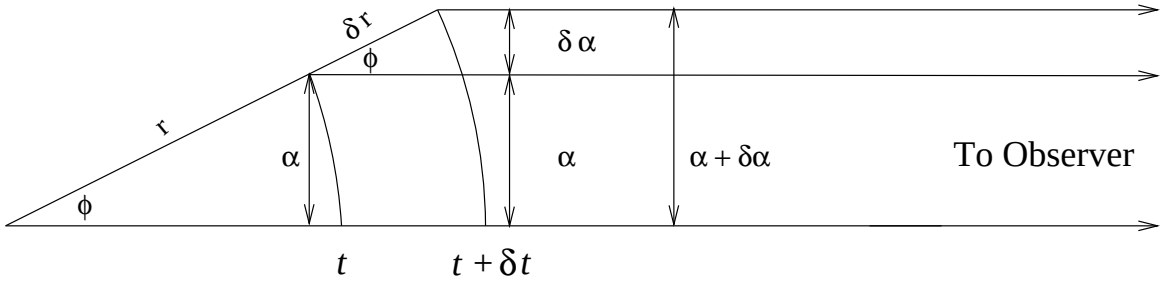

Figure 2. Geometries for a spherically-symmetric shell expanding at a fixed velocity, V. The observed angular radius of a spot on the shell as it expands is shown by the values α, $\alpha + \delta\alpha$.

shell fades, the expanding spot on this second shell becomes visible.

The difference in apparent speeds for the two flares can be explained if we imagine the flares to be running into some ambient medium and imparting momentum. A graph of the distance travelled by the shell against time is shown in Figure 3. If both shells are expanding at the same initial rate, we would observe flare 1 to travel unhindered, then run into an object that slows it down. After a time t we would have observed it to have travelled a distance A at an average velocity $v_1 = A/t$. During this deceleration, if the shell pushes back the ambient medium it will have allowed flare 2 to expand a greater distance before being decelerated. For the second flare the initial speed is the same, but the shell travels further, to B before it is slowed down. On the same time-scale, t, the average speed will have increased to $v_2 = B/t$. The maximum shell expansion speed occurs when a previous shell has pushed the braking medium out far enough so we do not see deceleration within the time scale t. This is the true expansion velocity of the shell.

In this model a shell apparently expanding at $16c$ produces a superluminal expansion of an elliptical area which then fades and appears to contract superluminally. The model accounts for the elliptical shape and the lower minor axis velocities. Illumination of a subsequent shell produces the next expansion and contraction phase. This shell is expected to travel further before retardation and have a higher average speed.

5 CONCLUSIONS

We have considered a number of models which attempt to explain the superluminal expansions and contractions observed in Cygnus X-3, and the observed elliptical shape. The latter two features are the most difficult to model. The two most successful models are a) the propagating photon pattern model and b) the model in which expanding shells of material are illuminated by an off-axis jet or beam of radiation.

ACKNOWLEDGEMENTS

We would like to thank Pete Taylor and Tim Ash for useful comments during the development of the models presented here. RNO and SJN acknowledge the support of PPARC studentships.

REFERENCES

Giacconi R., Gorenstein P., Gursky H., Waters J.R., 1967, ApJ, 148, L119

Mirabel I.F., Rodríguez L.F., 1994, Nat, 371, 46

Newell S.J., 1996, PhD Thesis, University of Manchester

Newell S.J., Garrett M.A., Spencer R.E., 1996, Vistas in Astronomy, in press

Rybicki G.B., Lightman A.P., 1979, Radiative processes in astrophysics, Wiley

Spencer R.E., Swinney R.W., Johnston K.J., Hjellming R.M., 1986, ApJ, 309, 694

Tingay S.J. et al., 1995, Nat, 374, 141

Waltman E.B., Ghigo F.D., Johnston K.J., Foster R.S., Rielder R.L., Spencer J.H., 1995, AJ, 110, 290

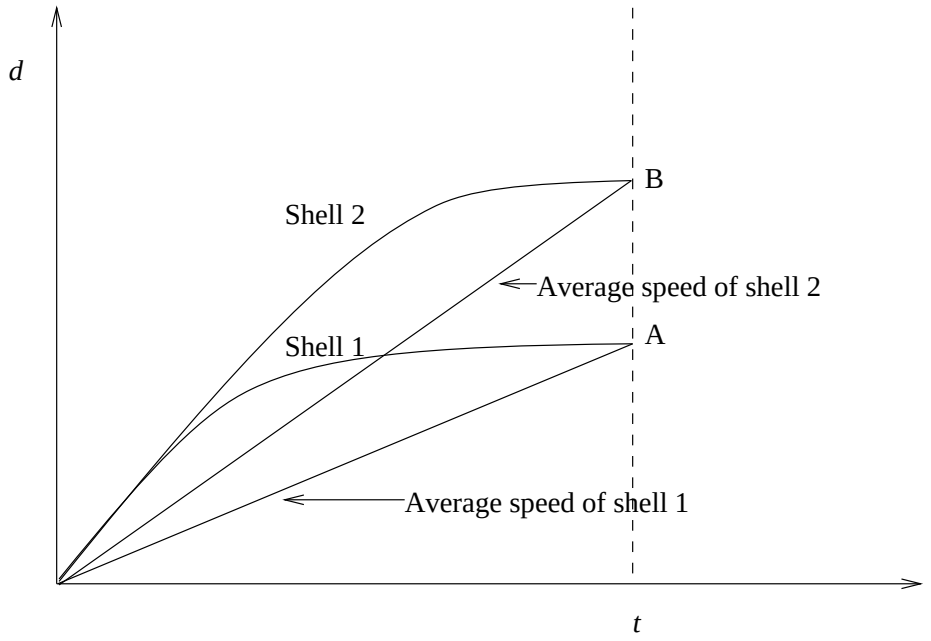

Figure 3. Shell expansions based on a constant initial speed for two shells. Shell 1 travels to a distance A before it is halted by some braking medium. Flare 1 moves the braking medium back a bit so shell 2 travels out further before being decelerated and thus has a higher average speed. The distance between A and B is approximately 900 $R_{\odot}$.